Covid-19 Detection by Wavelet Entropy and Artificial Bee Colony

Jia-Ji Wang[1], Yangrong Pei[2], Liam O'Donnell[3], and Dimas Lima[4(✉)]

[1] School of Math and Information Technology, Jiangsu Second Normal University, Nanjing 210016, Jiangsu, People's Republic of China
[2] Huai'an Tongji Hospital, Huai'an 223000, Jiangsu, China
[3] School of Engineering, University of Limerick, Limerick, Ireland
[4] Department of Electrical Engineering, Federal University of Santa Catarina, Florianópolis 88040-900, Brazil
dimaslima@ieee.org

Abstract. Computer analysis of patients' lung CT images has become a popular and effective way to diagnose COVID-19 patients amid repeated and evolving outbreaks. In this paper, wavelet entropy is used to extract features from CT images and integrate the information of various scales, including the characteristic signals of signals with transient components. Combined with the artificial bee colony optimization algorithm, we used the advantages of fewer parameters and simpler calculation to find the optimal solution and confirm COVID-19 positive. The use of K-fold cross validation allows the data set to avoid overfitting and unbalanced data set partition in small cases. The experimental results were compared with those of WE + BBO, GLCM-SVM, GLCM-ELM and WE-Jaya. Experimental data show that this method achieves our initial expectation.

Keywords: Covid-19 detection · Wavelet entropy · Artificial bee colony

1 Introduction

With the spread of the SARS COV-2, the number of confirmed patients with COVID-19 is increasing rapidly and the number of deaths from severe cases is still on the rise [1]. Under these circumstances, hospitals have to take on more pressure and call on more resources, including drugs, manpower and equipment [2], to screen patients. COVID-19 is a respiratory disease caused by the new coronavirus SARS COV-2 [3].

In February 2020, WHO announced that the official name of this disease is COVID-19. In this name, CO stands for corona, VI for the virus, D for disease, and 19 is for the first outbreak year of that disease [4]. The majority of patients have the following respiratory tract symptoms, common clinical manifestations include fever, cough, expectoration, weakness of limbs, headache and other symptoms, and there are also patients without obvious symptoms [5–7]. However, it is not yet clear what symptoms and complications

J.-J. Wang and Y. Pei — Contributed equally to this paper

S.-H. Wang and Y.-D. Zhang (Eds.): ICMTEL 2022, LNICST 446, pp. 644–654, 2022.
https://doi.org/10.1007/978-3-031-18123-8_50

can occur long after contracting COVID-19 [8, 9]. To improve the efficiency of screening, we use Wavelet Entropy and Artificial Bee Colony model to diagnose COVID-19 images.

Some researchers have proposed some classical classification methods based on CT images of COVID-19 patients' lung. Research [10] uses CNN to detect COVID-19. By testing the performance of different pre-training models on CT tests [11], they found that a larger field data set could improve the testing capabilities of the models.

In this study [12], VGG16 and ResNet50 models are improved and optimized by using data expansion and fine-tuning techniques. The robustness and validity of the model were verified and tested using hierarchical 5-fold cross-validation. Finally, the model performs much better in binary classification than in multi-classification.

The research [13] proposed two deep learning structures including AlexNet architecture are proposed in this study. The input images are pre-segmented by ANN [14]. In one structure, BiLSTM layer was added, and time attribute was added, and the accuracy reached 98.7%.

In this study, we attempted to use Wavelet Entropy [15] and Artificial Bee Colony [16] to diagnose lung CT images of COVID-19 [17] patients. The following article is organized as follows. Section 2 shows the dataset we used. Section 3 describes our proposed approach. Section 4 discusses the experimental results. In the Sect. 5, we summarize the research of this paper.

2 Dataset

The data set we used consisted of three different types of patients and a healthy control group. All images have a resolution of 1024 × 1024 × 3. A total of 148 COVID-19 images and 148 healthy control (HC) images are obtained. Figure 1 shows two figures in the dataset we used [18].

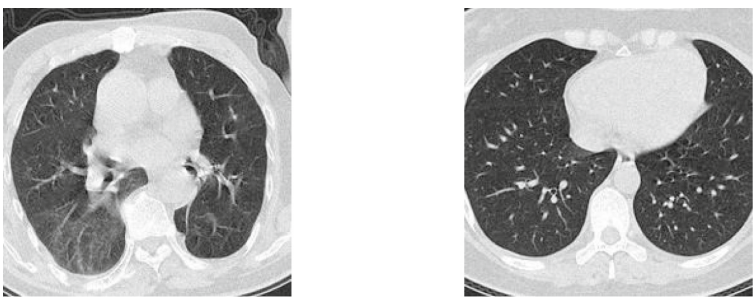

(a) COVID-19 (b) Healthy

Fig. 1. These two graphs are samples from the dataset

3 Methodology

3.1 Wavelet Entropy

The main factors to be considered in signal analysis are frequency, amplitude and phase. The main function of the Fourier transform [19] is to take a signal and decompose it into its constituent frequencies, converting the function into the form of multiple sinusoidal combinations, or e exponents [20, 21]. The signal is still the original signal essentially, but in a different way so that we can more analyze the frequency, amplitude, and phase components of a function intuitively. Therefore, after analyzing a complex signal through Fourier transform, its frequency [22], phase and amplitude components can be easily seen. It is a general analysis of the signal. The formula is:

$$F(\omega) = \int_{-\infty}^{\infty} f(t) e^{-i\omega t} dt \tag{1}$$

where ω represents frequency, t represents time.

But the Fourier transform has its own limitations. It can be seen from the Fourier transform formula that it is based on sine wave and its higher harmonics [23, 24] as the standard basis. If you need a good localization in the time domain, you need to analyze all the signals in the frequency domain [25–27]. If we want good results in one aspect, we have to give up the other one. Wavelet entropy changes the basis for the Fourier transform directly, replacing an infinite trig basis with a finite decaying wavelet basis [28, 29]. Thus, not only can we get the frequency, but also locate the time. The formula is as follows:

$$W(a, \tau) = \frac{1}{\sqrt{a}} \int_{-\infty}^{\infty} f(t) \psi \left(\frac{t - \tau}{a} \right) dt \tag{2}$$

where a is scale, τ is translation, ψ is parent wavelet function, and t is time.

That's obvious from the formula that the number of variables of wavelet transform is more than that of Fourier transform. In the wavelet transform, variable scale a controls the scaling of the wavelet function and variable translation τ controls the translation of the wavelet function. The scale a corresponds to frequency (inverse ratio) and the translation τ corresponds to time. As a more ideal tool, wavelet transform can provide a "time-frequency" window that changes with frequency, and transform the original fixed window size of Fourier transform into an adaptive window size for signal processing.

3.2 Feedforward Neural Network

Feedforward neural network [30] has a one-way multi-layer structure [31–33], and each neuron is arranged hierarchically, and each neuron is only connected with the previous neuron. The output of the previous layer is received and sent to the next layer [34–36], with no feedback between layers. A typical multilayer feedforward neural network is shown in Fig. 2.

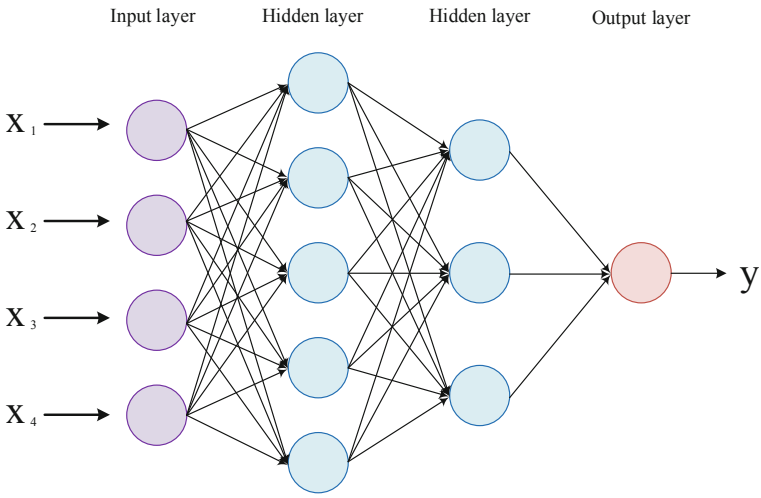

Fig. 2. A typical multilayer feedforward neural network

Feedforward neural network can be divided into single layer feedforward neural network [37] and multilayer feedforward neural network [38]. The single-layer feedforward neural network contains only one output layer, and the output value can be obtained directly by multiplying the input value by the weight value [39–41]. The multilayer feedforward neural network includes a input layer, one or more hidden layers and a output layer, which is relatively complex. Each layer of neurons is completely connected to the next layer of neurons, and there is no same-layer connection or cross-layer connection between neurons. Common feedforward neural networks include perceptron network [42], BP network [43] and so on.

3.3 Artificial Bee Validation

Artificial bee colony algorithm is an optimization method proposed by Karaboga in 2005 [44], which imitated bee behavior and has fast convergence speed. This method is similar to that after each worker bee finds the optimal solution, the colony is also displayed as the global optimal solution [45, 46]. In the basic ABC algorithm, artificial bee colony consists of three types of individuals: employed bees, onlooker bees and scout bees. Randomly generate feasible solution equal to the number of employed bees during initialization. Since each food source x_m is a feasible solution, each feasible solution containing n variables. It's a vector.(x_{mi}, $m = 1, 2\ldots SN$, $i = 1, 2\ldots n$).

The initialization formula is as follows:

$$x_{mi} = l_i + rand(0, 1) * (u_i - l_i), \tag{3}$$

where u_i means the maximum boundary values of x_{mi} and l_i means the minimum boundary values of x_{mi}.

Each employed bees corresponds to a certain feasible solution that already exists, and the field of nearby feasible solution is searched in the iteration. Employed bees continue to search for new feasible solutions near existing ones. The formula for finding new food sources is as follows:

$$v_{mi} = x_{mi} + \phi_{mi}(x_{mi} - x_{ki}) \tag{4}$$

The x_k is a random food source, i also is random, ϕ is a random number between $[-a, a]$. When a new feasible solutions is found, the fitness of the feasible solution is estimated [47–49] and the greedy selection is used to select between old and new food sources. The fitness calculation formula is as follows:

$$fit_m(x_m) = \begin{cases} \frac{1}{1+f_{m(x_m)}} & \text{if } f_{m(x_m)} \geq 0 \\ 1 + abs\left(f_{m(x_m)}\right) & \text{if } f_{m(x_m)} < 0 \end{cases} \tag{5}$$

where f_m is the objective function of the feasible solution x_m.

Scout bees use roulette to choose possible solutions based on the information brought back to the hive by the employed bees. The p_m formula for the probability of following bees choosing a food source is as follows:

$$p_m = \frac{fit_m(x_m)}{\sum_{m=1}^{SN} fit_m(x_m)} \tag{6}$$

If the feasible solution is still not improved after several updates, the feasible solution will be gave up, and the employed bee is turned into the scout bee to continue to randomly search for new feasible solutions.

3.4 K-fold Cross Validation

The total data set can be divided into training set and test set. K-fold cross Validation, a replacement-free resampling technique, can be used when the sample size is insufficient. In order to test the effectiveness of the algorithm, K-fold cross Validation randomly divides the total data set into K parts to make the best use of every piece of data in the data set, and takes out one package as the test set each time, and the remaining K-1 packages for training. The Fig. 3 shows the workflow of the K-fold method.

After k times, and these k models and performance evaluation were averaged to obtain the average performance. In many cases, K is 10. If the training set is relatively small, you can increase the K value. If the data set is large, reducing k value can reduce the refitting on different folds and the computational burden of model evaluation.

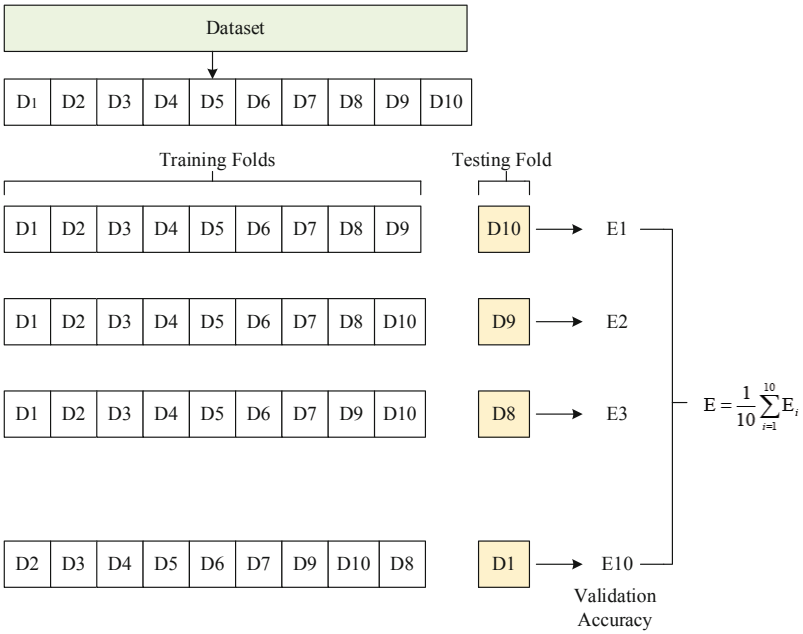

Fig. 3. The workflow of the K-fold method

4 Experience Results and Discussion

4.1 WE Results

Figure 4 shows an example of a level 4 decomposition of a biorthogonal decomposition. Wavelet transform divides the image into low-frequency part which changes slowly and high-frequency part which changes quickly. The upper left corner of Fig. 4(a) is the low-frequency information image of the input image obtained after the first-level wavelet transform, which is the frame and contour of the image. The other three images in Fig. 4(a) (located in the upper right corner, lower left corner and lower right corner) are the high-frequency information of the input image, reflecting the details of the input image. The upper sampling in the wavelet is the interval zero insertion, which aims to reconstruct the signal. The lower sampling introduced in the wavelet is the interval sampling of the signal. The edge lengths of the four self-band maps are universal for the input, and the purpose is to compress and store the information. The input image in Fig. 4(b) is the low-frequency information image in Fig. 4(a). Three images (upper right corner, lower left corner and lower right corner of Fig. 4(b)) are obtained after transformation similar to first-level wavelet transform. Figure 4(c) and Fig. 4(d) are obtained after the recursive operations.

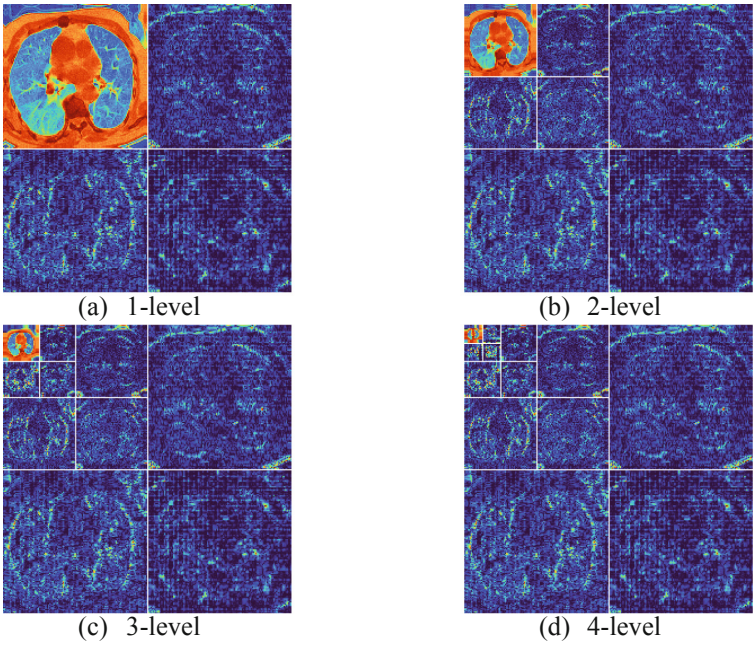

Fig. 4. An example of a level 4 decomposition of a biorthogonal decomposition

4.2 Statistical Results

The feature extraction method used in Wavelet Entropy and Artificial Bee Colony is wavelet entropy, the classifier is FNN, and 10 times 10-fold cross validation reports unbiased performance. The data show that the experiment achieves good performance (Table 1). The average sensitivity was 75.14 ± 1.93, the specificity was 77.30 ± 2.45, the precision was 76.85 ± 1.72, the accuracy was 76.22 ± 0.96, the F1 score was 75.95 ± 0.95, the Matthews correlation coefficient was 52.48 ± 1.95, and the feature mutual information of 75.97 ± 0.95.

4.3 Comparison to State-of the Art Approaches

To understand the level of this method proposed by us, we consulted relevant literature and compared our experimental data with the experimental data of the current more advanced method, as shown in Table 2. As the results in the Table 2, the Sen, Acc, F1, MCC and FMI data of this method are the best among these methods. ABC algorithm has strong ability to find the optimal solution globally and fast convergence speed. However, similar to the gradient descent method, when approaching the global optimal solution, it may fall into the local optimal solution, and the later search speed slows down in the subsequent search. According to these characteristics, ABC algorithm is applicable to solving the multivariable function optimization problems.

Table 1. Results of 10-fold cross-validation

Run	Sen	Spc	Prc	Acc	F1	MCC	FMI
1	75.68	77.70	77.24	76.69	76.45	53.39	76.45
2	72.97	82.43	80.60	77.70	76.60	55.65	76.69
3	76.35	75.00	75.33	75.68	75.84	51.36	75.84
4	77.70	75.00	75.66	76.35	76.67	52.72	76.67
5	74.32	77.03	76.39	75.68	75.34	51.37	75.35
6	75.00	76.35	76.03	75.68	75.51	51.36	75.51
7	71.62	78.38	76.81	75.00	74.13	50.11	74.17
8	75.68	74.32	74.67	75.00	75.17	50.00	75.17
9	74.32	79.73	78.57	77.03	76.39	54.13	76.42
10	77.70	77.03	77.18	77.36	77.44	54.73	77.44
Mean + SD	75.14 ± 1.93	77.30 ± 2.45	76.85 ± 1.72	76.22 ± 0.96	75.95 ± 0.95	52.48 ± 1.95	75.97 ± 0.95

Table 2. The results are compared with the existing advanced methods

Method	Sen	Spc	Prc	Acc	F1	MCC	FMI
WE + BBO [50]	72.84 ± 3.00	75.00 ± 1.99	74.47 ± 1.20	73.92 ± 1.18	73.61 ± 1.57	47.89 ± 2.34	73.63 ± 1.56
GLCM-SVM [51]	72.03 ± 2.94	78.04 ± 1.72	76.66 ± 1.07	75.03 ± 1.12	74.24 ± 1.57	50.20 ± 2.17	74.29 ± 1.53
GLCM-ELM [52]	74.19 ± 2.74	77.81 ± 2.03	77.01 ± 1.29	76.00 ± 0.98	75.54 ± 1.31	52.08 ± 1.95	75.57 ± 1.28
WE-Jaya [18]	73.31 ± 2.26	78.11 ± 1.92	77.03 ± 1.35	75.71 ± 1.04	75.10 ± 1.23	51.51 ± 2.07	75.14 ± 1.22
WE-ABC (Ours)	75.14 ± 1.93	77.30 ± 2.45	76.85 ± 1.72	76.22 ± 0.96	75.95 ± 0.95	52.48 ± 1.95	75.97 ± 0.95

5 Conclusions

The use of computer analysis of CT images for classification is attracting more and more attention. People realized that this was a way to save a lot of medical and human resources, and to reduce unnecessary contact with patients and reduce the risk of infection. Combined with wavelet entropy and artificial bee colony algorithm, this study proves that the model has improved the classification of CT images. The data show that the results are relatively ideal. This method has not been applied in other medical image classification tasks so far. In the future, we will apply this method to different types of medical images to continuously verify, optimize and improve the performance of this method. We believe that after continuous experiments, the application scope of

this method will be more extensive, suitable for the classification and diagnosis of various diseases, and improve the efficiency and accuracy of diagnosis, so as to face more challenges in the future.

References

1. Lufler, R.S., et al.: The glass ceiling thickens: the impact of COVID-19 on academic medicine faculty in the United States. Med. Educ. Online **27**(1), 2058314 (2022)
2. Jerzak, M., Szafarowska, M.: Preliminary results for personalized therapy in pregnant women with polycystic ovary syndrome during the COVID-19 pandemic. Arch. Immunol. Ther. Exp. **70**(1), 1–7 (2022). https://doi.org/10.1007/s00005-022-00650-z
3. Santana, J.C., et al.: Complicações em testes para COVID-19 com swab nasal: relatos de caso. Revista de Medicina **101**(2) (2022)
4. Acter, T., et al.: Evolution of severe acute respiratory syndrome coronavirus 2 (SARS-CoV-2) as coronavirus disease 2019 (COVID-19) pandemic: a global health emergency. Sci. Total Environ. **730**, 138996 (2020)
5. Zhang, X.: Diagnosis of COVID-19 pneumonia via a novel deep learning architecture. J. Comput. Sci. Technol. **37**(2), 330–343 (2022)
6. Yang, L.: EDNC: ensemble deep neural network for Covid-19 recognition. Tomography **8**(2), 869–890 (2022)
7. Guo, X.: A survey on machine learning in COVID-19 diagnosis. Comput. Model. Eng. Sci. **130**(1), 23–71 (2022)
8. Balasubramanian, P., et al.: Outcomes in patients with mild COVID-19 treated with casirivimab and imdevimab or bamlanivimab-a single-center retrospective cohort study in the bronx. Infect. Dis. Clin. Pract. **30**(3), e1128 (2022)
9. Hashimoto, K., et al.: Severe infectious acute respiratory failure mimicking COVID-19 in a healthy adolescent. Respirology Case Rep. **10**(4), e0933 (2022)
10. Zhao, W., et al.: Deep learning for COVID-19 detection based on CT images. Sci. Rep. **11**(1), 14353 (2021)
11. Khan, M.A.: VISPNN: VGG-inspired stochastic pooling neural network. Comput. Mater. Continua **70**, 3081–3097 (2022)
12. Mishra, N.K., et al.: Automated detection of COVID-19 from CT scan using convolutional neural network. Biocybern. Biomed. Eng. **41**(2), 572–588 (2021)
13. Aslan, M.F., et al.: CNN-based transfer learning-BiLSTM network: a novel approach for COVID-19 infection detection. Appl. Soft Comput. **98**, 106912 (2021)
14. Shanbehzadeh, M., et al.: Developing an artificial neural network for detecting COVID-19 disease. J. Educ. Health Prom. **11** (2022)
15. Wang, W., et al.: Covid-19 diagnosis by WE-SAJ. Syst. Sci. Control Eng. **10**, 325–335 (2022)
16. Jacob, I.J., et al.: Artificial bee colony optimization algorithm for enhancing routing in wireless networks. J. Artif. Intell. **3**(01), 62–71 (2021)
17. Govindaraj, V.: Deep rank-based average pooling network for Covid-19 recognition. Comput. Mater. Continua **70**, 2797–2813 (2022)
18. Wang, W.: Covid-19 detection by wavelet entropy and jaya. Lecture Notes in Computer Science, vol. 12836, pp. 499–508 (2021)
19. Anaya-Isaza, A., et al.: Fourier transform-based data augmentation in deep learning for diabetic foot thermograph classification. Biocybern. Biomed. Eng. **42**, 437–452 (2022)
20. Sahabuddin, M., et al.: Co-movement and causality dynamics linkages between conventional and Islamic stock indexes in Bangladesh: a wavelet analysis. Cogent Bus. Manag. **9**(1), 2034233 (2022)

21. Meenpal, A., Majumder, S.: Image content based secure reversible data hiding scheme using block scrambling and integer wavelet transform. Sādhanā **47**(2), 1–17 (2022). https://doi.org/10.1007/s12046-022-01828-z
22. Khani, M.E., et al.: Translation-invariant zero-phase wavelet methods for feature extraction in terahertz time-domain spectroscopy. Sensors **22**(6), 2305 (2022)
23. Fang, Y., et al.: Optimal control over high-order-harmonic ellipticity in two-color cross-linearly-polarized laser fields. Phys. Rev. A **103**(3), 033116 (2021)
24. Wu, X.: Diagnosis of COVID-19 by wavelet renyi entropy and three-segment biogeography-based optimization. Int. J. Comput. Intell. Syst. **13**(1), 1332–1344 (2020)
25. Biswas, A., et al.: Revisiting OD-stretching dynamics of methanol-d(4), ethanol-d(6) and dilute HOD/H2O mixture with predefined potentials and wavelet transform spectra. Chem. Phys. **553**, 111385 (2022)
26. Messer, P.K., Henß, A.-K., Lamb, D.C., Wintterlin, J.: A multiscale wavelet algorithm for atom tracking in STM movies. New J. Phys. **24**(3), 033016 (2022). https://doi.org/10.1088/1367-2630/ac4ad5
27. Chia, C., et al.: Interpretable classification of bacterial Raman spectra with Knockoff wavelets. IEEE J. Biomed. Health Inform. **26**(2), 740–748 (2022)
28. Utudee, S., Maleewong, M.: Multi-resolution wavelet basis for solving steady forced Korteweg–de Vries model. J. Inequalities Appl. **2021**(1), 1–14 (2021). https://doi.org/10.1186/s13660-021-02696-7
29. Jiang, X.: Multiple sclerosis recognition by biorthogonal wavelet features and fitness-scaled adaptive genetic algorithm. Front. Neurosci. **15**(1098), 737785 (2021)
30. Yee, J., et al.: Image features of a splashing drop on a solid surface extracted using a feedforward neural network. Phys. Fluids **34**(1), 013317 (2022)
31. Nimmanterdwong, P., et al.: Artificial neural network prediction of transport properties of novel MPDL-based solvents for post combustion carbon capture. Energy Rep. **8**, 88–94 (2022)
32. Ullah, W., et al.: Artificial intelligence of things-assisted two-stream neural network for anomaly detection in surveillance big video data. Future Gener. Comput. Syst. Int. J. Escience **129**, 286–297 (2022)
33. Christensen, O., et al.: A neural network approach for property determination of molecular solar cell candidates. J. Phys. Chem. A **126**(10), 1681–1688 (2022)
34. Yan, Y., Yao, X.-J., Wang, S.-H., Zhang, Y.-D.: A survey of computer-aided tumor diagnosis based on convolutional neural network. Biology **10**(11), 1084 (2021). https://doi.org/10.3390/biology10111084
35. Wang, S.-H., Satapathy, S.C., Anderson, D., Chen, S.-X., Zhang, Y.-D., Deep fractional max pooling neural network for COVID-19 recognition. Front. Pub. Health **9** (2021). https://doi.org/10.3389/fpubh.2021.726144
36. Zhang, Y.-D., Satapathy, S.C., Wu, D., Guttery, D.S., Górriz, J.M., Wang, S.-H.: Improving ductal carcinoma in situ classification by convolutional neural network with exponential linear unit and rank-based weighted pooling. Complex Intell. Syst. **7**(3), 1295–1310 (2020). https://doi.org/10.1007/s40747-020-00218-4
37. Koçak, Y., et al.: New activation functions for single layer feedforward neural network. Expert Syst. Appl. **164**, 113977 (2021)
38. Rizk-Allah, R.M., Hassanien, A.E.: COVID-19 forecasting based on an improved interior search algorithm and multilayer feed-forward neural network. In: Hassanien, A.E., Bhatnagar, R., Snášel, V., Yasin Shams, M. (eds.) Medical Informatics and Bioimaging Using Artificial Intelligence. SCI, vol. 1005, pp. 129–152. Springer, Cham (2022). https://doi.org/10.1007/978-3-030-91103-4_8

39. Hajiahmadi, M., Zarei, M., Khataee, A.: An effective natural mineral-catalyzed heterogeneous electro-Fenton method for degradation of an antineoplastic drug: modeling by a neural network. Chemosphere **291**, 132810 (2022). https://doi.org/10.1016/j.chemosphere.2021.132810
40. Ankobea-Ansah, K., et al.: A hybrid physics-based and stochastic neural network model structure for diesel engine combustion events. Vehicles **4**(1), 259–296 (2022)
41. Goudarzi, F., Hedayatiaghmashhadi, A., Kazemi, A., Fürst, C.: Optimal location of water quality monitoring stations using an artificial neural network modeling in the Qarah-Chay River Basin, Iran. Water **14**(6), 870 (2022). https://doi.org/10.3390/w14060870
42. Radhakrishnan, S., et al.: Multilayer perceptron neural network model development for mechanical ventilator parameters prediction by real time system learning. Biomed. Sign. Process. Control **71**, 103170 (2022)
43. Chen, L., Jagota, V., Kumar, A.: Research on optimization of scientific research performance management based on BP neural network. Int. J. Syst. Assurance Eng. Manag., 1–102021).https://doi.org/10.1007/s13198-021-01263-z
44. Karaboga, D.: An idea based on honey bee swarm for numerical optimization. Technical report-tr06, Erciyes university, engineering faculty, computer (2005)
45. Wu, L.: Magnetic resonance brain image classification by an improved artificial bee colony algorithm. Prog. Electromagn. Res. **116**, 65–79 (2011)
46. Wu, L.: Optimal multi-level thresholding based on maximum tsallis entropy via an artificial bee colony approach. Entropy **13**(4), 841–859 (2011)
47. Khababa, G., et al.: An extended artificial bee colony with local search for solving the skyline-based web services composition under interval QoS properties. J. Intell. Fuzzy Syst. **42**(4), 3855–3870 (2022)
48. Mahmoodabadi, M.J., et al.: Optimal design of an adaptive robust controller using a multi-objective artificial bee colony algorithm for an inverted pendulum system. Trans. Can. Soc. Mech. Eng. **46**(1), 89–102 (2022)
49. Rahimi, A.M., et al.: Artificial bee colony algorithm with proposed discrete nearest neighborhood algorithm for discrete optimization problems. Jurnal Kejuruteraan **33**(4), 1087–1095 (2021)
50. Yao, X., Han, J.: COVID-19 detection via wavelet entropy and biogeography-based optimization. In: Santosh, K.C., Joshi, A. (eds.) COVID-19: Prediction, Decision-Making, and its Impacts. LNDECT, vol. 60, pp. 69–76. Springer, Singapore (2021). https://doi.org/10.1007/978-981-15-9682-7_8
51. Chen, Y.: Covid-19 classification based on gray-level co-occurrence matrix and support vector machine. In: Santosh, K.C., Joshi, A. (eds.) COVID-19: Prediction, Decision-Making, and its Impacts. LNDECT, vol. 60, pp. 47–55. Springer, Singapore (2021). https://doi.org/10.1007/978-981-15-9682-7_6
52. Pi, P.: Gray level co-occurrence matrix and extreme learning machine for Covid-19 diagnosis. Int. J. Cognitive Comput. Eng. **2**, 93–103 (2021)